CA^{2+}-dependent interaction of the trpl cation channel and calmodulin

Claudia Trost, Andrea Marquart, Stephanie Zimmer, Stephan Philipp, Adolfo Cavalié, Veit Flockerzi*

Institut für Pharmakologie und Toxikologie, Universität des Saarlandes, D-66421 Homburg, Germany

Received 23 March 1999; received in revised form 16 April 1999

Abstract The transient receptor potential-like ion channel from *Drosophila melanogaster* was originally identified as a calmodulin binding protein (Philips et al., 1992) involved in the dipterian phototransduction process. We used a series of fusion proteins and an epitope expression library of transient receptor potential-like fusion proteins to characterize calmodulin binding regions in the transient receptor potential-like channel through the use of [^{125}I]calmodulin and biotinylated calmodulin and identified two distinct sites at the C-terminus of the transient receptor potential-like ion channel. Calmodulin binding site 1, predicted from searching of the primary structure for amphiphilic helices (Philips et al., 1992), covers a 16 amino acid sequence (S_{710}–I_{725}) and could only be detected through biotinylated calmodulin. Calmodulin binding site 2 comprises at least 13 amino acids (K_{859}ETAKERFQRVAR$_{871}$) and binds both [^{125}I]calmodulin and biotinylated calmodulin. Both sites (i) bind calmodulin at least in a one to one stoichiometry, (ii) differ in their affinity for calmodulin revealing apparent K_i values of 12.3 nM (calmodulin binding site 1) and 1.7 nM (calmodulin binding site 2), respectively, (iii) bind calmodulin only in the presence of Ca^{2+} with 50% of site 1 and site 2, respectively, occupied by calmodulin in the presence of 0.1 μM (calmodulin binding site 1) and 3.3 μM Ca^{2+} (calmodulin binding site 2) and give evidence that (iv) a Ca^{2+}-calmodulin-dependent mechanism contributes to transient receptor potential-like cation channel modulation when expressed in CHO cells.

Key words: Calcium; Calmodulin; Epitope library; Fusion protein; Ion channel (trpl)

1. Introduction

Two photoreceptor cell-specific gene products have been isolated from *Drosophila melanogaster* which have been implicated to be light sensitive ion channels involved in the invertebrate phototransduction process [2,3]. The transient receptor potential (*trp*) gene product is a protein of 1275 amino acids [4,5] with multiple transmembrane domains and when expressed in vitro, leads to an increased Ca^{2+} conductance which is activated after the depletion of intracellular Ca^{2+} stores by inositol 1,4,5-trisphosphate ($InsP_3$) or thapsigargin [6–9]. The transient receptor potential-like (*trpl*) gene is 49% identical to TRP over the N-terminal 850 amino acids [1] and encodes a non-selective cation channel [10,11,12].

The trpl gene was initially isolated in a screen for calmoduline (CaM) binding proteins from a *Drosophila* head cDNA expression library [1]. As a result of searching the amino acid sequence for amphiphilic α-helices, TRPL was originally postulated to contain two CaM binding sites in its C-terminal domain [1] and in the following, it was shown that a synthetic peptide representing the predicted CaM binding site 1 (CaMBS1) of TRPL binds CaM in a Ca^{2+}-dependent manner [13]. The predicted CaM binding site 2 (CaMBS2) was localized to amino acids 809–825 [1,14], although there is experimental evidence that CaMBS2 is localized within a 43 amino acid sequence from residue 853 to residue 895 of TRPL [13]. This second site was shown to bind the Ca^{2+}-free form of CaM [13]. In contrast to these experiments, the results of recent in vivo studies implicate that TRPL light-activated channels are modulated by Ca^{2+}-CaM [15] and that in intact *Drosophila* photoreceptor cells, TRPL channels bind CaM only in the presence of Ca^{2+} [15]. These findings prompted us to characterize in detail the distinct localization of CaM binding sequences present in TRPL and their potential Ca^{2+}-dependency. We now report Ca^{2+}-dependent CaM binding to the TRPL protein employing three experimental approaches, that are CaM overlay assays, mobility shift assays and CaM-sepharose chromatography. In addition, we mapped CaMBS2 to 13 amino acid residues within the TRPL protein and show that both sites, CaMBS1 and CaMBS2, differ in their affinities for CaM and bind CaM at least in a one to one stoichiometry. Using a somatic cell line stably expressing the TRPL cation channel [12], we also show that the CaM antagonist calmidazolium inhibits the Ca^{2+}-dependent activation of TRPL currents indicating TRPL channel modulation by intracellular Ca^{2+} via CaM.

2. Materials and methods

2.1. Materials

Purified phosphodiesterase (PDE1A2) was generously provided by W.K. Sonnenburg and J.A. Beavo, Department of Pharmacology, University of Washington (Seattle, WA, USA), the *Drosophila* trpl cDNA by M. Phillips, Department of Genetics, University of Melbourne. Various materials and reagents were obtained from the following suppliers: 2.8-[^{3}H]cGMP from Amersham; [α-^{35}S]dATP (1000 Ci/mmol) and ^{125}I-Bolton Hunter-labelled CaM (83.4 μCi/μg) from DuPont NEN; nitrocellulose sheets from Schleicher and Schuell; pGEX-2T and CaM-sepharose from Pharmacia Biotech; bovine brain CaM, biotinylated bovine brain CaM, calmidazolium and streptavidin alkaline phosphatase conjugate from Calbiochem; SDS-PAGE standards, *Crotulus atrox* snake venom, DEAE sephadex A25 anion exchange resin and cGMP from Sigma. Peptides corresponding to amino acid residues CaMBS1-(710–725)-SVKWVIRIF-RKSSKTI, CaMBS2-(854–875)-PSKPAKETAKERFQRVARTVLL, CaMBS2-(859–871)-KETAKERFQRVAR and B42d-(7–20)-LPTGV-SSGVHASSA of the TRPL protein were synthesized at the Institut

*Corresponding author. Fax: (49) (6841) 166402.
E-mail: veit.flockerzi@med-rz.uni-sb.de

Abbreviations: CaM, calmodulin; CaMBS, calmodulin binding site; CHO, Chinese hamster ovary; HEDTA, *N*-hydroxyethyletyhlenediaminetriacetic acid; $InsP_3$, inositol 1,4,5-trisphosphate; PDE, 3′, 5′-cyclic-nucleotide phosphodiesterase; Trp, transient receptor potential; Trpl, transient receptor potential-like

PII: S0014-5793(99)00588-8

für Pharmakologie und Toxikologie, Technische Universität München. All other reagents were of the highest purity grade available.

2.2. Constructs for expression of glutathion S-transferase (GST) fusion proteins

All recombinant DNA manipulations were carried out using standard procedures [16]. Fusion protein epitopes of TRPL [1] were constructed by amplifying base pairs 2278–2625 (a), 2392–3525 (b) and 1945–2496 (c) covering amino acid residues 709–825 (a), 747н1124 (b) and 598н782 (c), respectively, with the following primers: 5′-CGG GAT CCG TCA AGT GGG TCA TC-3′, 5′-CGG AAT TCT CAC GCC ACC TGG AAG CCC TT-3′, 5′-CGG GAT CCC TGG TTT GGC GAT AT-3′, 5′-CGG AAT TCT TAG TTT CGA TGC TTT GG-3′, 5′-CGG AAT TCC TAA CGC ATC GTA TTG ATC TC-3′ and 5′-CGG GAT CCC ACG GAG ACT CCT GCA TG-3′. The resulting PCR products were digested with *Bam*HI and *Eco*RI, subcloned in the pGEX-2T vector and sequenced on both strands by the dideoxy chain termination method using [α-^{35}S]dATP [17]. Recombinant pGEX vectors were introduced into *Escherichia coli* BL21 cells and protein expression was carried out as described previously [18]. Afterwards, proteins were separated electrophoretically in 12% SDS-polyacrylamide gels according to [19].

2.3. Protein transfer to nitrocellulose and CaM overlay experiments

The resolved proteins were transferred to nitrocellulose membranes (0.45 μm) at 0.8 mA/cm^2 for 80 min. For detection of [^{125}I]CaM binding proteins, the nitrocellulose membranes were incubated with 10 mM imidazole, pH 7.4, 150 mM KCl, 1 mM $CaCl_2$, 0.2% Tween 20 (buffer A) and 5% non-fat dry milk for 1 h at 21°C, followed by overlay with [^{125}I]CaM (3.5×10^6 cpm/ml buffer A and 5% dry milk) for 4 h at 21°C. Membranes were washed with buffer A three times for 10 min at 21°C. Bound [^{125}I]CaM binding proteins were visualized by autoradiography. For detection of proteins binding biotinylated CaM, the nitrocellulose membranes were incubated with 50 mM Tris-HCl, pH 7.4, 150 mM NaCl, 50 mM $MgCl_2$, 500 μM $CaCl_2$ (buffer B) and 10% non-fat dry milk for 1 h, followed by overlay with biotinylated CaM (100 ng/ml buffer B and 10% dry milk) for 2 h at 21°C. The nitrocellulose membranes were washed three times for 10 min with buffer B and then incubated in the presence of streptavidin-alkaline phosphatase at a dilution of 1:1000 in buffer B for 30 min. The membranes were then washed three times for 10 min in buffer B followed by a wash in 100 mM Tris-HCl, pH 9.5, 100 mM NaCl, 50 mM $MgCl_2$ and 500 μM $CaCl_2$ (buffer C) and color was developed with nitro blue tetrazolium and 5-bromo-4-chloro-indolyl phosphate at 0.33 mg/ml and 0.175 mg/ml buffer C, respectively.

2.4. Construction and screening of a TRPL epitope library

Construction and screening of the TRPL epitope library was carried out as described previously [18,20,21] except that TRPL cDNA fragments of 50–150 bp length were electro-eluted. After construction and expression of T7 Gen10 TRPL fusion proteins, bacterial colonies were transferred on replica filters, lysed and denatured and then, the filters were blocked in buffer A containing 5% non-fat dry milk, washed twice with the same solution followed by an incubation in the presence of [^{125}I]CaM (3.5×10^6 cpm/ml buffer A and 5% dry milk) for 4–6 h at 21°C. After washing three times in buffer A, the filters were dried and exposed to a X-ray film (Hyperfim MP, Amersham). For isolation of single positive colonies, a re-screen was performed and cDNA inserts of positive clones were sequenced on both strands.

2.5. Phosphodiesterase assay

Phosphodiesterase assays in the presence or absence of synthetic TRPL peptides CaMBS1-(710–725), CaMBS2-(854–875), CaMBS2-(859–871) and B42d-(7–20) were carried out according to established procedures [22] with the 61 kDa bovine PDE1A2 CaM-stimulated cyclic nucleotide phosphodiesterase [23].

2.6. CaM-sepharose chromatography of synthetic peptides

30 nmol of synthetic peptides representing the CaM binding sites were dissolved in 250 μl buffer containing 50 mM Tris-HCl pH 7.3, 100 mM NaCl and the Ca^{2+} concentrations described ('Ca^{2+} buffer') or 5 mM EGTA ('Ca^{2+}-free buffer'), respectively, and then applied to 0.5 ml CaM-sepharose columns (~33 nmol CaM) pre-equilibrated in the same buffers. The Ca^{2+} concentrations between 0.01 and 10 μM were adjusted by adding EGTA or *N*-hydroxyethyletyhlenediaminetriacetic acid (HEDTA) according to Schoenmakers et al. [24]. The columns were washed with 5–10 ml of the respective Ca^{2+} buffer followed by a wash with the 'Ca^{2+}-free buffer' to elute residual bound peptides. All wash fractions were collected and the peptide concentrations determined by the BCA protein assay reagent kit (Pierce) using the respective peptides as standards.

2.7. Mobility shift assay to study binding of the peptide to Ca^{2+}-CaM

Mixtures of TRPL peptides and CaM fixed at 15 μM at different molar ratios were incubated in 50 mM Tris-HCl pH 7.3, 250 mM NaCl and either 1 mM $CaCl_2$ or 2 mM EGTA and aliquots comprising 3 μg CaM were separated on gradient gels containing 5–20% acrylamide and 375 mM Tris-HCl, pH 8.8, at 10 mA for 8–12 h at 4°C. After electrophoresis, the gel was stained with Coomassie blue.

2.8. Electrophysiological measurements

Current recordings from a Chinese hamster ovary (CHO) cell line stably expressing the TRPL cDNA [12] were carried out by using the patch-clamp technique in the whole-cell configuration [25]. Pipettes (Kimax: Kimble Products, Witz Scientific, OH, USA) were pulled to obtain resistances between 2.5 and 5 MW. The pipette solution contained 7 μM free Ca^{2+}, 110 mM CsCl, 5.5 mM $CaCl_2$, 3 mM $MgCl_2$, 10 mM EDTA and 5 mM HEPES, pH 7.2 (CsOH). Current measurements were performed in bath solutions containing 115 mM NaCl, 5 mM KCl, 10 mM $CaCl_2$, 2 mM $MgCl_2$, 5 mM HEPES, pH 7.4 (NaOH). Series resistances (R_s) and the whole-cell membrane capacitance (C_m) were read from the settings provided by the amplifier after cancellation of transients occurring in the whole-cell configuration. Only current recordings from experiments with >1 GW seal resistance and a R_s lower than 10 MW were pooled for statistical evaluations. Electronic compensation of about 50% was currently used to improve the charging time.

3. Results and discussion

3.1. Localization of two CaM binding sites

To identify CaM binding sites in TRPL, we constructed and expressed a number of GST fusion proteins that contain fragments of TRPL covering the C-terminal half of the protein (Fig. 1A). [^{125}I]CaM binding to these fusion proteins was examined by an overlay procedure (Fig. 1B). Strong [^{125}I]CaM binding was detected in fusion protein b and degradation products of protein b, but not in a and c. According to these results, the C-terminal 300 amino acids of TRPL appear to be sufficient to bind CaM but interestingly, they do not include the amino acid sequences S_{710}–R_{728} and R_{809}–A_{825}, originally predicted to represent CaM binding sites on the basis of sequence analysis [1].

In order to identify the precise localization of potential CaM binding sites within the complete TRPL protein, an epitope expression library of TRPL fusion proteins was constructed and screened with [^{125}I]CaM as probe. 12 independent clones were identified and isolated. Sequence analysis revealed that all clones contained cDNAs in the appropriate reading frame and encoded peptide sequences containing 17–46 amino acids (Fig. 1C). The smallest epitope sufficient to bind CaM was encoded by clone S15 (Fig. 1C), comprising 17 amino acids and extending from residue K_{859} to L_{875} of TRPL. Interestingly, it contained 13 residues (amino acids K_{859}–R_{871}) which were also included in the derived sequence of the 12 other clones isolated, indicating that this 13 amino acid sequence motif is sufficient for CaM binding. No clones were obtained encoding peptide sequences derived from other regions of the TRPL protein.

In previous studies, Warr and Kelly [13] gave evidence that biotinylated CaM binds to two CaM binding sites within TRPL covering amino acids 711–725 and a 43 amino acid

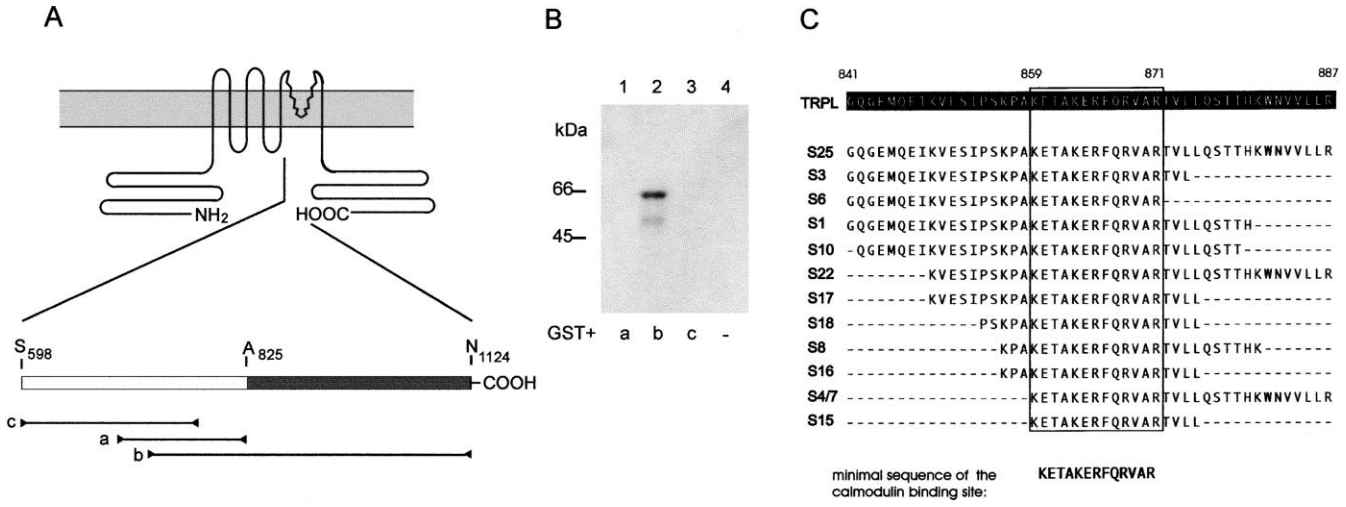

Fig. 1. Identification of CaM binding sites of TRPL. A: Model of transmembrane topology of TRPL including the putative pore region flanked by the putative fifth and sixth transmembrane segments is shown. Bar represents the C-terminal half of TRPL (S598–N1124) with the protein region responsible for CaM binding indicated (A825–N1124). B: Bacterial lysates representing 50 μg of protein and containing fusion proteins a (lane 1), b (lane 2) and c (lane 3) and GST (lane 4), respectively, were separated by SDS-PAGE, transferred to nitrocellulose membranes and overlaid with [^{125}I]CaM in the presence of 1 mM Ca^{2+}. [^{125}I]CaM binding (autoradiogram) occurs with GST fusion protein b, but not to a, c or GST control (−). C: Alignment of amino acid sequences of fusion TRPL epitopes as deduced from the 12 independent clones obtained by screening an epitope expression library of TRPL with [^{125}I]CaM. Boxed letters represent the common 13 amino acid residues (K859–R871) encoded by all clones and representing a minimal CaM binding site.

sequence (residues 853–895 of TRPL) which they called CaMBS1 and CaMBS2. The 13 amino acid peptide identified by screening the TRPL epitope library with [^{125}I]CaM in the present study is part of the 43 amino acid peptide identified by Warr and Kelly [13] and specifies further the amino acids of CaMBS2 necessary to bind CaM. However, CaMBS1 could not be detected using [^{125}I]CaM as probe. Therefore, fusion proteins c (GST fusion protein: $M_r \sim 51\,000$, Fig. 1B) and S25 (epitope library clone, T7 Gen10 fusion protein: $M_r \sim 40\,000$, Fig. 1C) supposed to contain CaMBS1 and CaMBS2, respectively, were expressed in *E. coli* and separated electrophoretically. Fig. 2A shows a Coomassie blue-stained gel of fusion proteins S25 (BS2, left lane) and c (BS1, right lane), respectively. Fig. 2B shows an autoradiograph of a blot prepared from a similar gel as in Fig. 2A, but overlaid with [^{125}I]CaM. Strong [^{125}I]CaM binding was detected in CaMBS2 (BS2) but not in CaMBS1 (BS1). In contrast, when a second blot of a similar gel was overlaid with biotinylated CaM, binding was detected in both fusion proteins (Fig. 2C). Obviously, the mode of interaction differed in that CaM binding of CaMBS1 could only be detected by biotinylated CaM whereas site 2 binds both, biotinylated CaM and [^{125}I]CaM. Iodination occurs predominantly at lysine residues of CaM [26,27] and the incorporation of ^{125}I apparently disturbs CaM binding to site 1.

3.2. Determination of the CaM-peptide complex stoichiometry in the presence of calcium

In order to quantify the interaction between the binding sites and Ca^{2+}-CaM, we synthesized two peptides, CaMBS1-(710–725) and CaMBS2-(854–875). Binding of the peptides to CaM was analyzed with a gel shift assay, in which a mixture of the respective peptide and CaM was run on a non-denaturing gel in the presence of Ca^{2+} (Fig. 3). In the absence of the peptides, there was a single band reflecting pure Ca^{2+}-CaM. At a ratio of CaMBS2-(854–875) to CaM of 0.25 or 0.5, two bands were visible on the gel (Fig. 3A), a Ca^{2+}-CaM band and another that migrated with a lower mobility, representing the peptide-Ca^{2+}-CaM complex. When the ratio of peptide to CaM was unity, the pure CaM band disappeared and the peptide-CaM complex band concurrently increased in intensity. At still higher ratios, no new bands appeared on the gel suggesting that multivalent complexes were absent. Removal of Ca^{2+} by EGTA in a control experiment (data not shown) abolished complex formation. These observations suggest that CaMBS2-(854–875) binds CaM with a one to one stoichiometry in a Ca^{2+}-dependent way. In contrast, using comparable experimental conditions, no peptide-CaM complex was observed using CaMBS1-(710–725) either in the absence or presence of Ca^{2+} (Fig. 3B). Similar results as in Fig. 3B were obtained after changing the experimental conditions including elongation of electrophoresis time, electrophoresis at lower

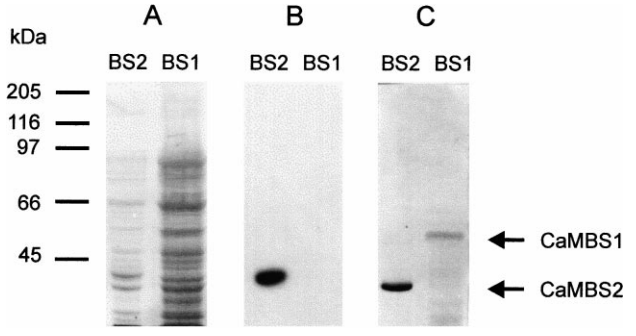

Fig. 2. Expression of fusion proteins containing CaMBS1 and CaMBS2 and detection of biotinylated CaM and [^{125}I]CaM binding. A: Coomassie blue staining of whole-cell lysates expressing fusion proteins S25 (10 μg, BS2) and c (100 μg, BS1) containing CaMBS2 and CaMBS1, respectively, separated by 8% SDS-PAGE. B: An autoradiograph of a blot from a gel similar to that presented in (A), but overlaid with [^{125}I]CaM in the presence of 1 mM Ca^{2+}. C: A blot from a gel similar to that presented in A but overlaid with biotinylated CaM in the presence of 1 mM Ca^{2+}. Arrows indicate positions of CaMBS1 (C) and CaMBS2 (B, C).

voltages or an increase of the length of the incubation time of CaMBS1-(710–725) and CaM in the absence or presence of Ca^{2+} prior to electrophoresis. These results suggest that CaMBS1-(710–725) is unable to interact directly with CaM under the conditions employed in these experiments.

3.3. Quantitation of binding affinities of peptide-CaM complexes

To get an estimate of the apparent potencies of CaM binding of the CaM binding sites CaMBS1 and CaMBS2, a competition assay using the PDE1A2 CaM-stimulated cyclic nucleotide phosphodiesterase was employed. PDE1A2 has a basal activity for cGMP hydrolysis and can be activated by CaM [23]. To determine which peptide most potently binds CaM, PDE1A2 was assayed in the presence of 4 nM CaM and peptide concentrations ranging between 100 pM and 10 μM (Fig. 4A). Peptide CaMBS2-(854–875) showed the strongest inhibition with an IC_{50} of 2.78 ± 0.27 nM. The peptide CaMBS2-(859–871) comprising the minimal CaM binding motif of 13 amino acids was less potent having an IC_{50} value of 340 ± 69 nM. Surprisingly, peptide CaMBS1-(710–725) which did not show complex formation with CaM in the mobility shift assay (Fig. 3B) now appears to bind to CaM. The peptide competed with PDE1A2 for CaM with an apparent IC_{50} value of 19.8 ± 2.3 nM. Peptide B42d-(7–20), covering amino acid residues 7–20 of TRPL was used as a negative control. There is only a slight decrease of enzyme activity in the presence of B42d-(7–20) (≤6%, Fig. 4A), indicating a specific interaction of CaMBS peptides, CaM and PDE1A2. K_i values according to the Cheng-Prusoff equation [28] were 12.3 ± 1.4, 1.7 ± 0.2 and 211 ± 43.3 nM for CaMBS1-(710–725), CaMBS2-(854–875) and CaMBS2-(859–871), respectively.

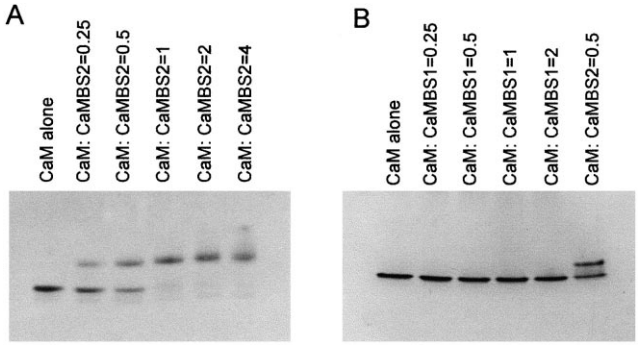

Fig. 3. Binding of the CaMBS2 and CaMBS1 peptides to Ca^{2+}-CaM studied in a gel mobility shift assay. Mixtures of peptides CaMBS2-(854–875) (A) and CaMBS1-(710–725) (B) and CaM at different molar ratios (with the CaM concentration fixed at 15 μM) were incubated in the presence of 1 mM Ca^{2+} for 30 min at 21°C. A portion of each mixture was then separated by non-denaturing polyacrylamide gel electrophoresis in the presence of 1 mM Ca^{2+} and proteins were stained by Coomassie blue. Being negatively charged, CaM migrated toward the positive pole in the bottom of the gel (A, lane 1). The complex formed (A, lanes 2–6 and B, lane 6) between CaMBS2-(854–875) and Ca^{2+}-CaM was stable during electrophoresis and migrated with a lower mobility. No mobility shift was observed in B (lanes 2–5) using different molar ratios of CaM and the CaMBS1-(710–725) peptide.

The inhibition of CaM-stimulated PDE1A2 activity by the synthetic peptides can be caused by either competition of peptides with PDE1A2 for CaM or a direct interaction of peptides with PDE1A2. Addition of peptides CaMBS1 or CaMBS2 at 100 nM inhibited the PDE activity stimulated with 3 nM CaM (Fig. 4B). However, no inhibition by the peptides was detected when an excess of CaM (240 nM) was used to activate the PDE, indicating that the inhibition ob-

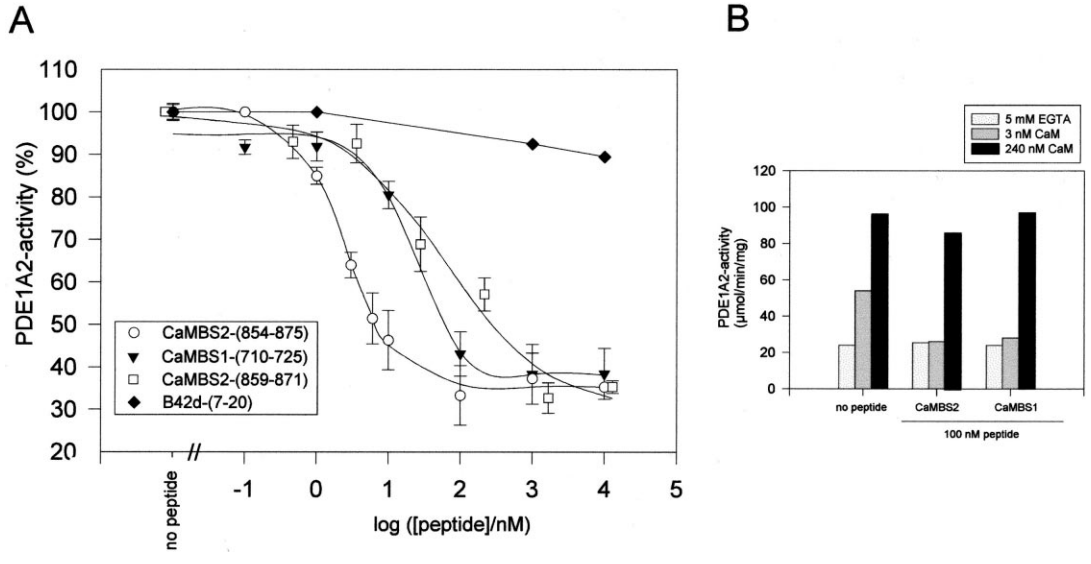

Fig. 4. A: inhibition potency of CaM-stimulated phosphodiesterase PDE1A2 activity by synthetic TRPL peptides. 2.44 nM of partially purified bovine PDE1A2 was assayed with 100 pM to 10 μM synthetic peptide CaMBS1-(710–725), CaMBS2-(854–875), CaMBS2-(859–871) or B42d-(7–20) in the presence of 0.2 mM $CaCl_2$ and 4 nM CaM. Enzyme activity is expressed as the percentage of CaM-stimulated PDE1A2 activity in the absence of synthetic peptides (activities ranges from 51 to 73 μmol/min/mg protein). Values are presented as the mean of three assays performed in triplicate. The IC_{50} values for peptides CaMBS1-(710–725), CaMBS2-(854–875) and $CaMBS2_{13}$ were 19.8 ± 2.3, 2.78 ± 0.27 and 340 ± 69 nM, respectively (x ± S.E.M). B: The ability of excess CaM to overcome inhibition of CaM-stimulated phosphodiesterase PDE1A2 activity by synthetic peptides CaMBS2 and CaMBS1. Partially purified PDE1A2 was assayed in the presence of either 5 mM EGTA (white bars), 0.2 mM $CaCl_2$ and 3 nM CaM (gray bars) or 0.2 mM $CaCl_2$ and 240 nM CaM (black bars) and either no peptide or 100 nM synthetic peptide CaMBS2 or CaMBS1. PDE1A2 activity is expressed as μmol cGMP hydrolyzed/min/mg of protein. Values are the mean of triplicate determinations. The S.E.M. (not shown) did not exceed 15% of the mean activity value.

served is due to competition of the peptides with PDE1A2 for CaM.

3.4. The effect of the Ca^{2+} concentration on CaM binding

The experiments shown so far demonstrate that peptides CaMBS1-(710–725), CaMBS2-(854–875) and CaMBS2-(859–871) bind CaM. Previously, it has been suggested that at least CaMBS2 binds the Ca^{2+}-free form of CaM, whereas CaMBS1 binds CaM in a Ca^{2+}-dependent fashion, requiring concentrations above 0.3–0.5 μM for CaM binding [13]. In these experiments [13], a peptide representing CaMBS1 and a fusion protein containing CaMBS2 were bound to CaM-sepharose in 100 μM Ca^{2+} and then washed in the presence of decreasing concentrations of Ca^{2+} [13]. We performed a similar experiment using the synthetic peptides CaMBS1-(710–725) and CaMBS2-(854–875) and the results obtained are summarized in Table 1. 91% of CaMBS1-(710–725) and 96% of CaMBS2-(854–875) bound to CaM-sepharose in the presence of 100 μM Ca^{2+}, even after extensive washing of the column with a Ca^{2+} containing buffer. However, both peptides are almost completely eluted by Ca^{2+}-free buffer (91% of bound CaMBS1 and 97% of CaMBS2) indicating that CaMBS2 as well as CaMBS1 bound CaM only in the presence of Ca^{2+} ions.

In an extension of this experiment, equal amounts of CaMBS1-(710–725) were bound to CaM-sepharose in the presence of 10 μM, 1 μM, 0.5 μM, 0.3 μM, 0.1 μM and in the absence of Ca^{2+}, respectively. After consecutive washes with the corresponding Ca^{2+} buffer and Ca^{2+}-free buffer, the peptide concentrations in the respective wash solutions were determined and the amount of bound peptide calculated. CaM binding to CaMBS1-(710–725) (Fig. 5A triangles) depends on the presence of Ca^{2+} and maximal binding occurs at a free Ca^{2+} concentration of 1 μM. At 0.1 μM Ca^{2+}, CaMBS1 is occupied by CaM at 50%. In these experiments, almost equal amounts of CaM-sepharose (33 nmol) and peptide (30 nmol) were employed and the results obtained indicate that CaMBS1 binds CaM at least in a one to one stoichiometry.

As has been demonstrated in the previous experiments employing CaM-sepharose, CaM binding to CaMBS2 depends on the presence of Ca^{2+}. To study the Ca^{2+}-dependent binding of CaM to CaMBS2 in detail, the fusion protein S25, containing CaMBS2 (Fig. 2C), was expressed in bacteria and an overlay with [^{125}I]CaM was performed. In the next step, the filter was incubated in the presence of [^{125}I]CaM and 100 μM Ca^{2+} and in the following, the filter was cut into pieces, repeatedly washed with buffers of various free Ca^{2+} concentrations and exposed to a X-ray film. The intensities of the signals indicating the amount of [^{125}I]CaM bound to CaMBS2 (Fig. 5B) were analyzed by a phosphoimager and blotted in Fig. 5A (CaMBS2, circles) against the free Ca^{2+} concentration. At a free Ca^{2+} concentration of 3.3 μM (mean of two experiments), 50% of CaMBS2 is occupied by [^{125}I]CaM. In summary, these experiments demonstrate that both sites within the TRPL channel protein bind CaM in a Ca^{2+}-dependent way although binding of CaM to CaMBS2 occurs at 33-fold higher Ca^{2+} concentrations than binding to CaMBS1.

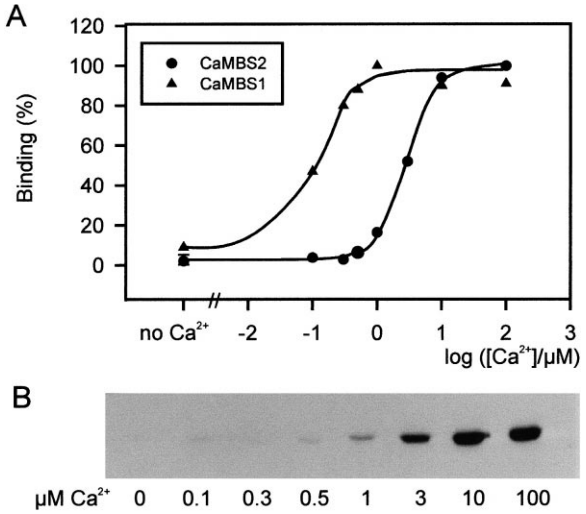

Fig. 5. The effect of the Ca^{2+} concentration on CaM binding to CaMBS1 and CaMBS2. A: Binding of CaM to CaMBS1 (triangles) or CaMBS2 (circles) in the absence and presence of increasing concentrations of Ca^{2+} is shown. CaM binding to CaMBS1 was examined by CaM-sepharose chromatography. B: [^{125}I]CaM binding to CaMBS2 was quantified by phosphoimager analysis. EC_{50} values of Ca^{2+}-dependent CaM binding to CaMBS1 and CaMBS2 were 0.1 and 3.3 μM, respectively (mean of two and three determinations, respectively). Binding is expressed as percentage of maximal binding.

Table 1
The effect of the Ca^{2+} concentration on CaM binding

Peptide	Buffer	Recovery from CaM-sepharose
CaMBS1-(710–725)	Ca^{2+}	9%
	Ca^{2+}-free	91%
CaMBS2-(854–875)	Ca^{2+}	4%
	Ca^{2+}-free	97%

30 nmol of peptide CaMBS1-(710–725) or peptid CaMBS2-(854–875), respectively, was bound to ~33 nmol CaM-sepharose, pre-equilibrated in 'Ca^{2+} buffer' (100 μM Ca^{2+}) or 'Ca^{2+}-free buffer' (5 mM EGTA), respectively. Columns were washed with 10–20 volumes of the appropriate buffer. The columns equilibrated with 'Ca^{2+} buffer' were additionally washed with 'Ca^{2+}-free buffer' to elute residual bound peptide. All wash fractions were collected and peptide concentrations were determined. Recovery of peptide in the wash fractions is expressed as the percentage of the total peptide applied (100%). Values represent means of two experiments.

3.5. Ca^{2+}-CaM-dependence of TRPL ion channel modulation

The CaM concentration within a cell is usually in the order of 1 μM, exceeding the K_i values of CaMBS1 (12.3 nM) and of CaMBS2 (1.7 nM) for CaM binding. In vivo, occupation of both binding sites by CaM should therefore depend on the cytosolic Ca^{2+} concentration which oscillates between 0.1–0.2 μM in a resting cell [29]. To study functional implications of Ca^{2+}-dependent CaM binding, the cDNA of the TRPL channel protein was stably expressed in a CHO cell line [12] and currents through TRPL channels were recorded with the patch-clamp technique in the whole-cell mode. In this expression system, TRPL currents are enhanced by a rise of the cytosolic Ca^{2+} concentration [12]. In contrast, while keeping cellular Ca^{2+} buffered with EGTA to < 50 nM, the TRPL current is not detectable [12]. Saturation of the channel activity occurs at 1.5–3 μM cytosolic Ca^{2+} with an apparent EC_{50} value of 450 nM for the Ca^{2+}-dependent activation [12]. This EC_{50} value is very similar to the Ca^{2+} concentrations of 0.1 and 3.3 μM required for CaM binding to TRPL (Fig.

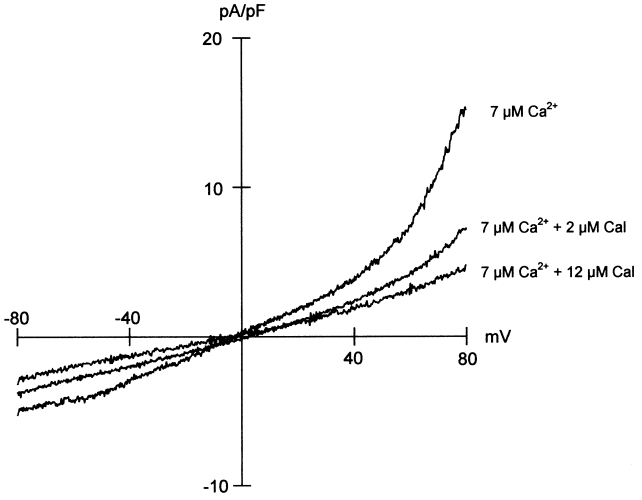

Fig. 6. Ca^{2+}-modulated TRPL currents and inhibition of the Ca^{2+}-dependent modulation by the CaM antagonist calmidazolium. The TRPL cDNA was stably expressed in CHO cells as described [10]. Original current recordings are shown without leak substraction. Previous to dialysis with 7 μM free Ca^{2+}, the cells were incubated for 30 min in the presence of 2 and 12 μM calmidazolium (Cal), respectively. The current densities at +60 mV (x ± S.E.M; *n*) from experiments performed in non-pretreated CHO (trpl) cells (5.7 ± 0.64 pA/pF; 8) and cells treated with 2 μM (4.35 ± 0.47 pA/pF; 10) and 12 μM calmidazolium (2.65 ± 0.33 pA/pF; 12).

5A), indicating that Ca^{2+}-dependent CaM binding modulates the TRPL channel function.

Fig. 6 shows traces of current densities elicited by voltage ramps from −80 to +80 mV. When CHO (trpl) cells [12] are incubated for 30 min in the presence of the CaM antagonist calmidazolium (2 μM), the enhancement of TRPL currents induced by dialysis of ~7 μM Ca^{2+} is markedly reduced (Fig. 6). By increasing the calmidazolium concentration to 12 μM, the TRPL channel activity is almost completely abolished since the current densities recorded under these conditions essentially reflect leak background levels of CHO cells (Fig. 6). Although the native channel may bind CaM in a different way than the isolated CaM binding sites, the Ca^{2+}-dependent modulation of the expressed TRPL channel [12] and the influence of the Ca^{2+} antagonist calmidazolium on this modulation (Fig. 6) argues in favor of a similar behavior of the CaM binding sites in the native channel compared with the behavior of the isolated sites.

In *Drosophila* phototransduction, CaM has been implicated to coordinate termination of the light response by modulating receptor and ion channel activity [15]. In addition to TRPL, other members of this signal transduction system are capable of CaM binding, such as TRP [30], the ryanodin receptor [31] or the inactivation no after-depolarization (*INAD*) gene product [30]. The finding that Ca^{2+}-dependent modulation of TRPL currents [12] is prevented in the presence of the CaM antagonist calmidazolium (Fig. 6) gives additional evidence for Ca^{2+}-CaM-dependent mechanisms underlying this process. In future experiments, it will be necessary to analyze the CaM function by expressing forms of the TRPL channel in which mutations have been introduced into the CaM binding sites, which have been characterized in this study. Furthermore, the mechanisms leading to inactivation of TRPL channels have not been defined and it was suggested [32] that the latter process might require another protein not necessarily present in the cell lines used so far for heterologous expression of TRPL cDNA. TRPL and TRP bind CaM and, in vivo, both proteins and possibly yet to be identified additional dipterian products of this gene family may assemble into homo- and/or heteromultimeric complexes [3,9,33]. It will be of interest to analyze the contribution of Ca^{2+}-CaM upon the function of such complexes. The knowledge of the Ca^{2+}-dependent CaM interaction with TRPL will facilitate this analysis.

Trp and trpl are archetypal members of a multigene family whose products share a structure that is highly conserved throughout evolution, from yeast to mammals. So far, at least seven mammalian TRP/TRPL homologous ion channels have been identified and one may speculate that some of them if not all are also capable of CaM binding.

Acknowledgements: We thank Drs W.K. Sonnenburg and J.A. Beavo, Department of Pharmacology, University of Washington, Seattle, for generously providing purified phosphodiesterase PDE1A2, Drs M. Phillips and L. Kelly, Department of Genetics, University of Melbourne, Parkville, Victoria, for generously providing the trpl cDNA. This work is part of the the Ph.D. thesis of C. Trost at the Technical University of Darmstadt, Germany, D-17. This work was supported by the Deutsche Forschungsgemeinschaft and the Fonds der Chemischen Industrie.

References

[1] Phillips, A., Bull, A. and Kelly, L. (1992) Neuron 8, 631–642.
[2] Peretz, A., Sandler, C., Kirschfeld, K., Hardie, R.C. and Minke, B. (1994) J. Gen. Physiol. 104, 1057–1077.
[3] Niemeyer, B.A., Suzuki, E., Scott, K., Jalink, K. and Zuker, C.S. (1996) Cell 85, 651–659.
[4] Montell, C. and Rubin, G.M. (1989) Neuron 2, 1313–1323.
[5] Wong, F., Schaefer, E.L., Roop, B.C., LaMendola, J.N., Johnson-Seaton, D. and Shao, D. (1989) Neuron 3, 81–94.
[6] Vaca, L., Sinkins, W.G., Hu, Y., Kunze, D.L. and Schilling, W.P. (1994) Am. J. Physiol. 267, C1501–C1504.
[7] Petersen, C.C.H., Berridge, M.J., Borgese, M.F. and Bennett, D.L. (1995) Biochem. J. 311, 41–44.
[8] Gillo, B., Chorna, I., Cohen, H., Cook, B., Manistersky, I., Chorev, M., Arnon, A., Pollock, J.A., Selinger, Z. and Minke, B. (1996) Proc. Natl. Acad. Sci. USA 93, (24) 14146–14151.
[9] Xu, X.-Z., Li, H.-S., Guggino, W.B. and Montell, C. (1997) Cell 89, 1155–1164.
[10] Harteneck, C., Obukhov, A.G., Zobel, A., Kalkbrenner, F. and Schultz, G. (1995) FEBS Lett. 358, 297–300.
[11] Hu, Y., Vaca, L., Zhu, X., Birnbaumer, L., Kunze, D.L. and Schilling, W.P. (1994) Biochem. Biophys. Res. Commun. 201, 1050–1056.
[12] Zimmer, S., Trost, C., Cavalié, A., Philipp, S. and Flockerzi, V. (1997) Arch. Pharmacol. 355, 238.
[13] Warr, C.G. and Kelly, L.E. (1996) Biochem. J. 314, 497–503.
[14] Lan, L., Brereton, H. and Barritt, G.J. (1998) Biochem. J. 330, 1149–1158.
[15] Scott, K., Sun, Y., Beckingham, K. and Zucker, C.S. (1997) Cell 91, 375–383.
[16] Sambrook, J., Fritsch, E.F. and Maniatis, T. (1989) Molecular Cloning: A Laboratory Manual, 2nd edn., Cold Spring Harbor Laboratory, Cold Spring Harbor, NY, USA.
[17] Sanger, F., Nicklen, S. and Coulson, A.R. (1977) Proc. Natl. Acad. Sci. USA 74, 5463–5467.
[18] Marquart, A. and Flockerzi, V. (1997) FEBS Lett. 407, 137–140.
[19] Laemmli, U.K. (1970) Nature 227, 680–685.
[20] Anderson, S. (1981) Nucleic Acids Res. 9, 3015–3027.
[21] Studier, F.W., Rosenberg, A.H., Dunn, J.J. and Dubendorff, J.W. (1990) Methods Enzymol. 185, 60–89.
[22] Sonnenburg, W.K., Seger, D. and Beavo, J.A. (1993) J. Biol. Chem. 268, 645–652.

[23] Sonnenburg, W.K., Seger, D., Kwak, K.S., Huang, J., Charbonneau, H. and Beavo, J.A. (1995) J. Biol. Chem. 270, 30989–31000.
[24] Schoenmakers, T.J.M., Visser, G.J., Flik, G. and Theuvenet, A.P.R. (1992) Biotechniques 12, 870–879.
[25] Hamill, O.P., Marty, A., Neher, E., Sakmann, B. and Sigworth, F.J. (1981) Pflug. Arch. 391, 85–100.
[26] Bolton, A.E. and Hunter, W.M. (1973) Biochem J. 133, 529–538.
[27] Van Eldik, L.J. (1988) Methods Enzymol. 159, 667–675.
[28] Cheng, Y.C. and Prusoff, W.H. (1973) Biochem. Pharmacol. 22, 3099–3108.
[29] Porter, J.A., Yu, M., Doberstein, S.K., Pollard, T.D. and Montell, C. (1993) Science 262, 1038–1042.
[30] Chevesich, J., Kreuz, A.J. and Montell, C. (1997) Neuron 18, 95–105.
[31] Takeshima, H., Nishi, M., Iwabe, N., Miyata, T., Hosoya, T., Masai, I. and Hotta, Y. (1994) FEBS Lett. 337, 81–87.
[32] Birnbaumer, L., Zhu, X., Jiang, M., Peyton, M., Vannier, B., Brown, D., Platano, D., Sadeghi, H., Stefani, E. and Birnbaumer, M. (1996) Proc. Natl. Acad. Sci. USA 93, 15195–15202.
[33] Tsunoda, S., Sierralta, J., Sun, Y., Bodner, R., Suzuki, E., Becker, A., Socolich, M. and Zuker, C.S. (1997) Nature 388, 243–249.